Structurally Integrated Piezoelectric Stack Absorbers for Nonstationary Disturbance Rejection

D. J. Belasco*, K. W. Wang, Structural Dynamics and Controls Lab, Penn State University, University Park, PA

Abstract

In this research, the active-passive piezoelectric absorber concept is investigated for nonstationary disturbance rejection and vibration control of complex structures, integrated with multiples of such absorber actuators. A scaled helicopter tailboom with four piezoelectric stack actuators is used as a testbed in this study. The stacks are connected to a power source through an inductor, and are actuated via a three-part control law. The first part, active inductance tuning, simulates a change in the apparent inductance allowing the absorbers to be effective over a wide frequency range. The second part, negative resistance, removes undesirable resistance (damping) from the absorber circuits thereby increasing the performance. The last action, active coupling, emulates an increase in the electro-mechanical coupling and adds to the robustness of the treatment. To expand the design from controlling a single-actuator simple system to a multi-actuator complex structure, the modal filter approach is used to identify the required feedback signals from the sensor readings. The effects of the differences and uncertainties of the different actuators on the system performance are also analyzed. It is shown that the active coupling action will significantly reduce the negative effects of the actuator uncertainties on the system performance. From examining the analytical and experimental results, the effects of the apparent electromechanical coupling factor are discussed and means to advance the investigation are identified.

1. Background and Overview

It has been known that piezoelectric shunts with resistance and inductance elements (Hagood and von Flowtow, 1991) can be designed as passive electromechanical absorbers for vibration control purposes. These systems can be tuned to provide modal damping (modal tuning) or to attenuate a harmonic disturbance (tonal tuning). Semi-active piezoelectric absorbers have also been proposed for suppressing harmonic excitations with varying frequency, a scenario that cannot be easily controlled using passive devices. However, these semi-active systems have limitations that restrict their applications. In a recent study, Morgan and Wang (2002) have developed a high performance active-passive alternative to the semi-active absorber that uses a combination of a passive electrical circuit and active control actions. While this new device has been shown, both analytically and experimentally, to be very effective for the suppression of harmonic disturbances with time-varying frequency, the focus has been on the control of single-actuator simple systems.

The objective of this research is to expand from the current active-passive absorber concept (Morgan and Wang, 2002) and examine its effectiveness on the control of more realistic complex structures integrated with multiple actuators. In this investigation, both analytical and experimental efforts are performed on a scaled helicopter tailboom testbed. The description of the testbed system is presented in Section 2. The actuator-structure system is controlled by a three-part algorithm with modal filter, as discussed in Section 3. The analytical and experimental results are illustrated and compared in Section 4.

2. Testbed System Description

The Penn State testbed structure, presented and discussed in (Heverly, et al, 2002), is a 0.3 scale model of a cantilevered helicopter tailboom section, based on the Apache AH64-A helicopter. A photograph and a diagram of the scaled tailboom model are shown in Figure 1 and Figure 2, respectively. Overall dimensions of the tailboom model are 81 inches long, 40 inches wide, and 38 inches high. The tailboom structure is fabricated with aluminum materials and a semi-monocoque construction technique. The boom section is a rectangular shaped and tapered box beam with 7 frame members, 8 perimeter stringers, and covered by 0.32-inch thick aluminum skin material. Four stringer members, one on each corner, are 0.75-inch aluminum angles. Four stringer members, one at the middle of each side, are 1.0 inch by 0.125 inch aluminum flat stock. The root end of the boom section is a 14 inch by 11 inch cross-section and tapers to 7 inch by 7 inch cross-section. The horizontal and vertical tail surfaces (stabilizers) of the tailboom structure are fabricated with 2 inch square aluminum tubing. All structural members are fastened with screws to permit efficient disassembly and modifications. The total weight of the tailboom model is 60 pounds, which includes 22.5 pounds of inertial mass at the free ends of the tail surfaces.

Report Documentation Page

Form Approved
OMB No. 0704-0188

1. REPORT DATE **00 JUN 2003**	2. REPORT TYPE **N/A**	3. DATES COVERED **-**	
4. TITLE AND SUBTITLE **Structurally Integrated Piezoelectric Stack Absorbers for Nonstationary Disturbance Rejection**		5a. CONTRACT NUMBER	
		5b. GRANT NUMBER	
		5c. PROGRAM ELEMENT NUMBER	
6. AUTHOR(S)		5d. PROJECT NUMBER	
		5e. TASK NUMBER	
		5f. WORK UNIT NUMBER	
7. PERFORMING ORGANIZATION NAME(S) AND ADDRESS(ES) **Structural Dynamics and Controls Lab, Penn State University, University Park, PA**		8. PERFORMING ORGANIZATION REPORT NUMBER	
9. SPONSORING/MONITORING AGENCY NAME(S) AND ADDRESS(ES)		10. SPONSOR/MONITOR'S ACRONYM(S)	
		11. SPONSOR/MONITOR'S REPORT NUMBER(S)	
12. DISTRIBUTION/AVAILABILITY STATEMENT **Approved for public release, distribution unlimited**			
13. SUPPLEMENTARY NOTES **See also ADM001697, ARO-44924.1-EG-CF, International Conference on Intelligent Materials (5th)(Smart Systems & Nanotechnology)., The original document contains color images.**			
14. ABSTRACT			
15. SUBJECT TERMS			

16. SECURITY CLASSIFICATION OF:			17. LIMITATION OF ABSTRACT **UU**	18. NUMBER OF PAGES **8**	19a. NAME OF RESPONSIBLE PERSON
a. REPORT **unclassified**	b. ABSTRACT **unclassified**	c. THIS PAGE **unclassified**			

Standard Form 298 (Rev. 8-98)
Prescribed by ANSI Std Z39-18

Figure 1 - Photograph of experimental test stand
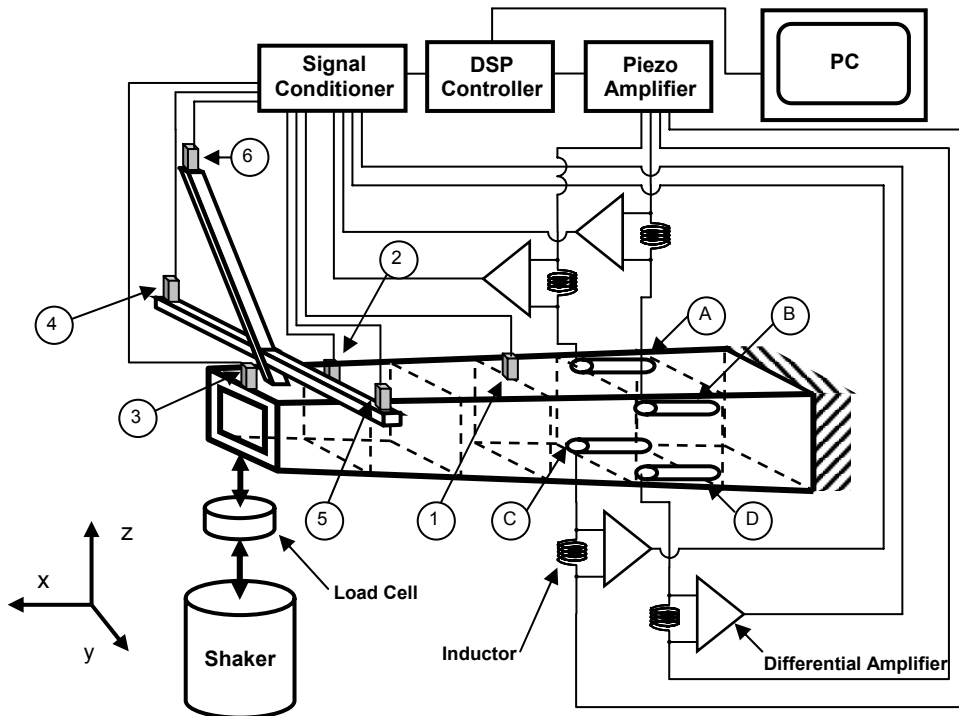
Figure 2 - Diagram of experimental testbed

Nine accelerometers are applied on the structure for modal filtering, at locations 1 through 6, as noted in Figure 2. There are six accelerometers, at locations 1 through 6, measuring the acceleration in the z-axis (the vertical direction, same axis as the excitation), two in the x-axis (extensional direction) at locations 4 and 6, and one in the y-axis (horizontal direction) at location 6. The one z-axis sensor located on the tip of the vertical stabilizer, (location 6), serves as the point of reference about which the vibration is to be minimized. Four piezoelectric stack actuators are installed at the corner stringers between the second and third frames of the tailboom, labeled A through D in Figure 2. Each of the actuators is connected to an inductance shunt circuit as well as an active voltage source, as shown in Figure 2. When high inductance is required, the

passive inductors could be implemented using op amp-based synthetic inductors, which can be modeled as passive inductance with inherent resistance. A load cell is installed in series with the stack actuator to monitor the loads generated by the actuators. Twenty strain gages are installed on the corner stringers near the actuator installation to monitor the dynamic strains of the structure. All sensor signals are fed through a signal-conditioning unit to a digital signal processor, and forwarded to a desktop PC for data collection.

An analytical finite element model of the scaled tailboom structure is constructed for design and analysis purposes (Heverly et al., 2001). The model contains 120 nodes and 267 elements with a total global degree-of-freedom of 536. The tailboom analytical model has been utilized to examine static deflections and system dynamic responses that are compared with experimentally measured data from the physical tailboom structure. Excellent agreement between the analytical models and the physical tailboom structure was achieved, in terms of their natural frequencies and static deflections (Heverly et al., 2002). More detail descriptions of the testbed and the analytical model can be found in (Heverly et al., 2001, 2002). The integrated structure-circuit equations with the additional circuitry are derived using Hamilton's principle and the linear theory of piezoelectricity (IEEE Standard, 1987). The complete derivation can be found in (Belasco, 2003).

3. Control Algorithm
It is assumed that the model of the structure and the piezoelectric absorbers can be obtained in the form shown below:

$$M\,\ddot{q} + C\,\dot{q} + Kq + Kc_1Q_1 + Kc_2Q_2 + Kc_3Q_3 + Kc_4Q_4 = F \qquad (1)$$

$$L_{p1}\,\ddot{Q}_1 + R_{p1}\,\dot{Q}_1 + \frac{1}{C_{p1}^S}Q_1 + Kc_1^T q = Vc_1 \qquad (2)$$

$$L_{p2}\,\ddot{Q}_2 + R_{p2}\,\dot{Q}_2 + \frac{1}{C_{p2}^S}Q_2 + Kc_2^T q = Vc_2 \qquad (3)$$

$$L_{p3}\,\ddot{Q}_3 + R_{p3}\,\dot{Q}_3 + \frac{1}{C_{p3}^S}Q_3 + Kc_3^T q = Vc_3 \qquad (4)$$

$$L_{p4}\,\ddot{Q}_4 + R_{p4}\,\dot{Q}_4 + \frac{1}{C_{p4}^S}Q_4 + Kc_4^T q = Vc_4 \qquad (5)$$

Equation 1 is the general structural equation in generalized coordinates, q, with mass, damping, stiffness, and forcing matrices respectively M, C, K, and F. The electro-mechanical coupling vectors Kc_i couples the structural equation to the ith circuit equation. The values in the Kc_i vectors are functions of the actuator materials property, the characteristics of the interface between the actuators and the structure, and the placement of the actuators, etc. Eqs. (2) to (5) are the circuit equations, where Q_i is the charge in the ith piezoelectric circuit, and L_{pi}, R_{pi}, $C_p^S{}_i$, and Vc_i, are the passive inductance, passive resistance, piezoelectric capacitance, and control voltage in the ith circuit, respectively.

Following the methodology developed in (Morgan and Wang, 2002), the passive inductance, L_{pi}, will be first tuned to create a frequency response function "notch" at a nominal frequency. Active actions (voltage inputs) will then be added to further enhance the performance of the treatment. Since there are four actuators, there are four circuit equations each with a charge input to the structural equation. The multiple circuit equations allow each of the actuators to be individually tuned. This creates an interesting steady state mistuning phenomenon. Due to uncertainties in the piezoelectric capacitance and shunt circuit inductance, an actuator could be mistuned to a different frequency (low vibration notch placement) away from the operating/excitation frequency. In the multiple actuator case every circuit creates its own notch. If each piezoelectric capacitance and circuit inductor is tuned to exactly the same frequency, all the notches will be on top of each other. However, if the actuators and circuits are mistuned, multiple notches will be created, which could affect the system performance. This concept is described further in Section 4.

Based on the model derived, an active controller is synthesized to specify the voltage inputs to the piezoelectric circuits. This control law consists of three parts, as described in the following sub-sections.

3.1 Active Inductor Tracking Action
The first control action is the active inductor tracking. The aim of this control scheme is to quickly tune the steady state notch to the current excitation frequency by adding or subtracting an apparent inductance term from the passive inductor via a control voltage input. The following equation shows the expression of the control voltage.

$$(Vc_{inductor})_i = -L_a(t)_i\,\ddot{Q}_i \qquad (6)$$

In the multiple actuator case, there is no closed form solution for optimal L_a tuning due to multiple coupling components in the structural equation. An active inductor tuning algorithm is developed using a quasi-steady-state assumption. It is assumed that the rate of frequency change in the excitation is slow enough that the circuit tuning can be done using a steady state approach and the transient vibration can be ignored. The frequency response function of the vertical stabilizer tip acceleration with a unit force shaker input is calculated at a given excitation frequency. This calculation will be performed for different absorber frequency values and the optimal absorber frequency that provides the minimum response of the vertical stabilizer will be selected through comparison of the results. In this study, we assume all four absorbers will be tuned to the same absorber frequency. The optimal L_a value is then derived from the optimal absorber frequency value. Note that the L_as will be different for different actuators, due to the differences between the four actuators and circuits (as explained in Section 4.1). The other feedback term necessary for inductor tracking is $\ddot{Q}$, the second derivative of the charge. This term is approximated by measuring the voltage across the passive inductor and dividing it by the passive inductance value.

3.2 Negative Resistance Action
The second control action is to add negative resistance to the circuit. For the treatment to be effective, it is usually desired to have very low damping (resistance) in the piezoelectric absorber. Therefore, it may be desirable to partially cancel the internal resistance of the passive inductor using an active negative resistance action. Reducing the passive resistance (damping) in the circuit will make the steady state frequency notch deeper, thus providing more vibration reduction. This negative resistance control can be implemented using the law shown below:

$$(Vc_{resistor})_i = (R_a)_i \, \dot{Q}_i \qquad (7)$$

This action is important since the passive inductors or the synthetic inductors can have significant inherent resistance.

3.3 Active Coupling Gain Action
The third control action is the active coupling action to enhance the apparent electromechanical coupling parameters in Eqs. (2)-(5). The control voltage is expressed as follows:

$$(Vc_{coupling})_i = -((G_{ac})_i - 1)Kc_i^T q \qquad (8)$$

Here, G_{ac} is the active coupling gain. This control is designed to emulate an increase in the coupling between the structure and the circuit. Increasing the coupling will widen the notch of the frequency response function around the tuned frequency, thereby increasing the robustness of the control action. As illustrated in Section 4.1, this will also reduce the negative effect of circuitry mistuning that might occur, which is especially important for the case with multiple mistuned actuators.

Given Eqs. (6)-(8), the overall control voltage for the ith circuit can be expressed as

$$Vc_i = (Vc_{inductor})_i + (Vc_{resistor})_i + (Vc_{coupling})_i \qquad (9)$$

3.4 Modal Filter Synthesis for Active Coupling Gain Synthesis

The challenge in implementing the active coupling action is to obtain the correct estimation of q. In order to estimate the modal displacement, a modal filter (Meirovitch et al, 1985) is implemented. Modal filtering uses the expansion theorem to approximate the modal coordinates. An appropriate expansion function is selected and multiplied by a discrete number of sensor (accelerometer) signals. This multiplication yields the respective modal acceleration of the structure. Since an accurate finite element model of the tailboom exists, the eigenvectors are selected as the expansion functions for the respective modes to be identified. Preliminary modal acceleration data are found by simulating a sine sweep excitation, through the relevant frequencies, on the analytical model. The rms values of the modal acceleration signals are compared to find the modes that are most important in the given frequency range. The modes with the highest vibration levels are chosen to be estimated by the modal filter. Theoretically, suitable sensor locations can be chosen using the energy term defined in Eq. (10) (Kammer, 1991),

$$KE_{in} = V_{in} \sum_{j=1}^{dof} M_{ij} V_{jn} \qquad (10)$$

KE_{in} represents the kinetic energy of the ith degree of freedom at the nth mode, V_{in} is the ith value in the nth eigenvector, M_{ij} is the mass matrix value in the ith row and jth column, V_{jn} is the jth value in the nth eigenvector, and dof denotes the number of structure degrees of freedom. Using this approach, the sensors should be placed at the degrees of freedom associated with the high kinetic energy values for the modes of interest. In practice, the nine sensors implemented are the pre-built-in accelerometers with their locations defined in Section 2. Through evaluating via Eq. (10), most of these sensor locations provide high kinetic energy for the modes of interest. Therefore, these accelerometers are used as sensors in the experimental

and analytical implementation of the control law. The accelerometer signals are used as input for the modal filters, as seen in Eq. (11). The output of the filter, the modal acceleration, is then numerically integrated twice to obtain the required modal displacement signal.

$$\ddot{q} = V_{red}^T \, \ddot{x}_{red}$$ (11)

Equation (11) shows the modal filter implementation, $\ddot{x}_{red}$ is an s by 1 acceleration vector measured at the sensor locations, where s is the number of sensors on the structure. V_{red}^T is the m by s modal filter matrix, the m rows of the matrix are comprised of s eigenvector values corresponding to the sensor locations. $\ddot{q}$ is the resulting m by 1 vector of the modal accelerations of the structure.

4. Results and Discussions

This section presents the analysis and experimental results obtained in this investigation. Through integrating the control law with the system model, computer simulation is first used to evaluate the system performance. The analysis uses the results from the modal filters and the voltage measurements across the inductors as feedback signals. The goal is to lower the vibration level at the tip of the vertical stabilizer when a time varying frequency excitation is introduced. The primary concern is around the first bending natural frequency, approximately 13.88 Hz.

4.1. Inductor mistuning

Due to variations (uncertainties) among the different piezoelectric stacks, the absorber inductors have to be tuned individually. However, because of the sensitivity and accuracy of the inductance tuning, it is very difficult to tune all the absorbers to the same frequency. Table 1 lists the capacitance of the actuators used, the passive inductance required to tune them exactly to the nominal frequency (13.88 Hz), and the inductance that can be achieved by the synthetic inductors used in the tests. Since the precision necessary to achieve exact tuning is not attainable, there will be inherent mistuning in the system. Further contributing to the mistuning is the changing of system parameters and environment over time.

The best way to study the mistuning effects is to examine the steady state tuning of the inductors. As mentioned, all the piezoelectric stacks have different capacitance values, each requiring a different and precisely tuned inductance. Here we assume no resistance and no active actions are applied. As seen in Figure 3(a), when the passive inductors are tuned exactly, there is a single notch at the nominal frequency (13.88 Hz). But with very slight inductor mistuning of 0.37%, -0.96%, 1.14%, and 5.59%, there are noticeable multiple notches, none of which are tuned to the correct frequency. In this mistuned example, with the mistuning percentages given by the experimental data, the vibration amplitude at the nominal frequency is almost as high as the structure without any treatment, the baseline case. Since the mistuning is very small and uncertain, it is difficult to use the active inductance action (normally also has small errors and uncertainties) to correct the differences.

Because the active coupling action is known to widen the frequency response notch and increase the robustness of the system, its effect on the mistuning is examined. In Figure 3(b), similar scenarios are presented as shown in Figure 3(a), but with active coupling action added. As illustrated in Figure 3(b), the active coupling action increases the width of all four notches and therefore "smoothes" out the response. Comparing the cases with and without mistuning, one can see that the active coupling action can indeed eliminate the undesirable effect of mistuning and enhance the robustness of the treatment.

Table 1 - Actuator and inductor properties

| Actuator Location	Capacitance (µF)	Desired Inductance (H)	Achieved Inductance (H)	Resistance (Ω)
A	17.73	7.2818	7.3085	49
B	19.23	6.7164	6.6517	37
C	17.87	7.2265	7.3085	128
D	18.73	6.8948	6.5091	74
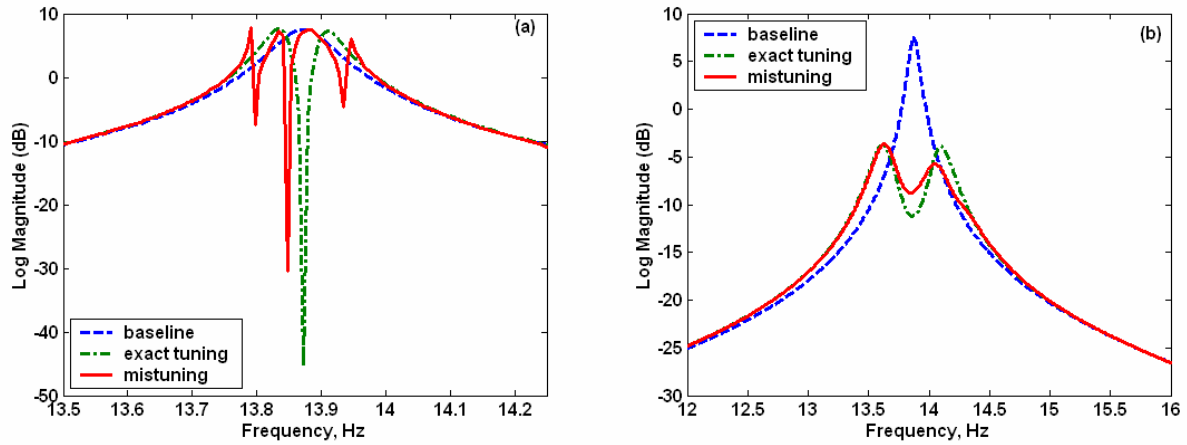
Figure 3 - Frequency response functions. Baseline curve – structural response without treatment. Other curves – (a) without active coupling; and (b) with active coupling

4.2. Vibration Control Results

To evaluate the effectiveness of the proposed treatment, a spin-up scenario is being analyzed numerically and examined experimentally. A chirp excitation is provided by the shaker on the tailboom testbed, simulating the spin-up condition, has an initial frequency of 1 Hz and a final frequency of 17 Hz. Two different chirp speeds are tested: 1 Hz/s, and 0.4 Hz/s. The absorber control is initiated at when the chirp frequency reached 9.5 Hz and remained on until 17 Hz.

Figure 4 illustrates the structural time response envelope (acceleration) of the tip of the vertical stabilizer. The baseline case is the structure without any control treatment. It is clear that the active-passive absorbers are very effective in suppressing the structural vibration when compared to the baseline, ending up with over 80% reduction in the peak amplitude for both the spin-up rates. When the system is evaluated experimentally (Figure 5), the improvement over the baseline is not as dramatic as shown in the analysis. However, it is still clear that active-passive absorber treatment can reduce the structural vibration amplitude under external excitation with varying frequency. The difference between the analytical and experimental results is due to the fact that the electromechanical coupling factors (Kc_i in Eqs. (1)-(5)) are smaller than predicted by the finite element model.
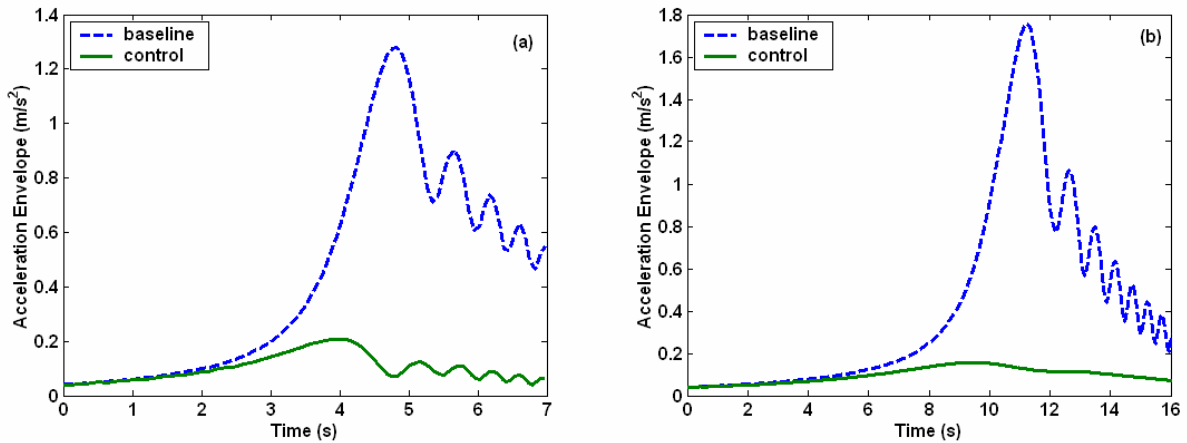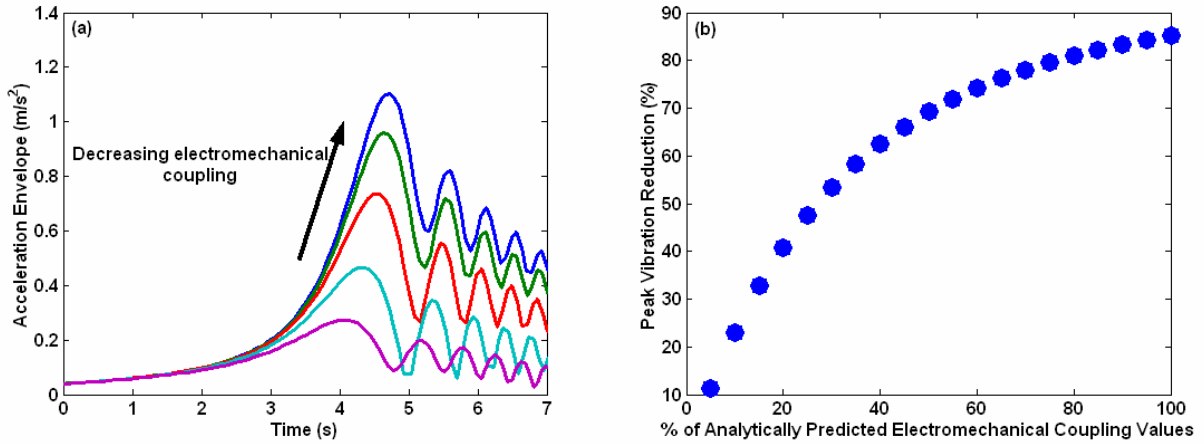

Figure 4 - Analytical acceleration envelopes for chirp excitation with rates of (a) 1 Hz/s and (b) 0.4 Hz/s
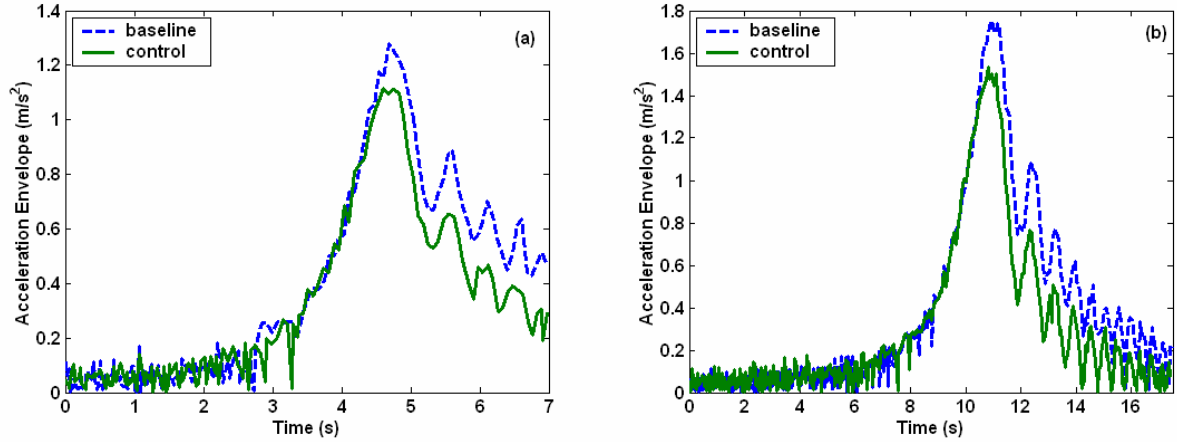
Figure 5 - Experimental acceleration envelopes for chirp excitation with rates of (a) 1 Hz/s and (b) 0.4 Hz/s

Figure 6(a) is a plot of numerical simulations of the structural response as a function of the electromechanical coupling factors. Note that here we assume that the Kc_i in the control law (Eq. (8)) is always the original value predicted by the analytical finite element model. That is, the control law is designed without knowledge of the variations or modeling errors of the coupling factors. It is readily seen that decreasing the actual value of the electromechanical coupling factors has a negative impact on the control performance and that the system response will differ significantly as compared to the original prediction. A similar conclusion can be observed from Figure 6(b), which illustrates the vibration reduction percentage (comparing the peak vibration amplitude of the controlled system with that of the baseline without treatment) as a function of the actual electromechanical coupling factor.

Figure 6 – (a) Analytical acceleration envelopes for varied electromechanical coupling values. (b) Peak vibration percentage reduction versus percent of analytically predicted electromechanical coupling values

Based on these observations, future investigations will focus on two major issues: one is to improve the model accuracy in predicting the system response; the second is to explore means to enhance system performance in the experiment.

Currently the piezoelectric stacks are rigidly attached to the structure on one end while the other end is attached with a ball joint. The ball joints prevent the stacks from experiencing potentially damaging bending moments. The present analytical model represents both joints as rigid connections. However, the ball joints add a sufficient amount of "play" to make the rigid connection assumption improper and create electromechanical coupling values that are lower than analytically predicted. A better model of this piezoelectric actuator-structure interface will be developed. A further search of different types of connection joints that can provide better and stronger interface will also be conducted.

In theory, the absorber performance could also be improved by increasing the active coupling gain G_{aci} to much larger values than currently used, even if the original electromechanical coupling factors are low. However, such an approach cannot be realized with the present hardware. The op amps used in the synthetic inductor constructions limit the control voltage to +/-

10V. Due to the circuitry architecture, the active control voltage values are therefore restricted by the op amp limitation. Using high voltage op amps or custom manufactured inductors will allow a more aggressive active action be implemented and enhance the performance.

5. Summary

The active-passive piezoelectric absorber concept is investigated for nonstationary disturbance rejection of complex structures integrated with multiples of such absorber actuators. A scaled helicopter tailboom with four piezoelectric stack actuators is used as a testbed. The stacks are connected to a power source through an inductor, and are actuated via a three-part active control law. To expand the design from controlling a single-actuator simple system to a multi-actuator complex structure, the modal filter approach is used to identify the required feedback signals from the sensor readings. The effects of the variations and uncertainties of the different actuators on the system performance are also analyzed. It is shown that the active coupling action will significantly reduce the negative effects of the actuator uncertainties on the system performance. The analysis results show that the multiple active-passive piezoelectric absorbers can suppress vibration very effectively. While the test results also show that the active-passive absorbers can control structural vibration, the improvement is not as dramatic as predicted analytically. From examining the differences between the analytical and experimental results, it is observed that improving the apparent electromechanical coupling factor could enhance the system performance significantly. Future research issues are identified to further advance the investigation, which include developing a better model of the piezoelectric actuator-structure interface; developing different types of connection joints that can provide a better interface and provide stronger electromechanical coupling; and using high voltage op amps or custom manufactured inductors that will allow the implementation of more aggressive active actions.

Acknowledgments

References

Belasco, D. J., 2003, Master's Thesis, The Pennsylvania State University

Hagood, N. W. and von Flowtow, A., 1991, "Damping of structural vibrations with piezoelectric materials and passive electrical networks," *Journal of Sound and Vibration*, Vol. 146 No. 2, pp. 243-268

Heverly, D., Wang, K. W., and Smith, E. C., 2001, "An optimal actuator placement methodology for active control of helicopter airframe vibrations," *American Helicopter Society Journal*, 46 (4), pp.251-261.

Heverly, D., Wang, K. W., and Smith, E. C., 2002, "Optimal actuator placement and active structure design for control of helicopter airframe vibrations," *Proc. of 58ᵗʰ AHS Forum.*

"IEEE Standard on Piezoelectricity", ANSI/IEEE STD 176-1987

Kammer, D., 1991, "Sensor placement for on-orbit modal identification and correlation of large space structures," *Journal of Guidance, Control, and Dynamics*, Vol. 14, No. 2, pp. 251-259

Meirovitch, L. and Baruh H., 1985, "The implementation of modal filters for control of structures," *Journal of Guidance, Control, and Dynamics*, Vol. 8, No. 6, pp. 707-716

Morgan, R. A. and Wang, K. W., 2002, "An active-passive piezoelectric absorber for structural vibration control under harmonic excitations with time-varying frequency, Part 1: Algorithm development and analysis, Part 2: Experimental validation and parametric study." *Journal of Vibration and Acoustics, Transactions of the ASME*, Vol. 124, No. 1, pp. 77-89.